DOI 10.1007/s10891-020-02262-w
Journal of Engineering Physics and Thermophysics, Vol. 93, No. 6, November, 2020

APPLICATION OF AN INTEGRAL NUMERICAL TECHNIQUE FOR A TEMPERATURE-DEPENDENT THERMAL CONDUCTIVITY FIN WITH INTERNAL HEAT GENERATION

O. O. Onyejekwe, G. Tamiru, T. Amha, F. Habtamu, Y. Demiss, N. Alemseged, and B. Mengistu

UDC 536.2.001

A numerical study of convective heat transfer in a longitudinal fin with temperature-dependent thermal conductivity and internal heat generation is undertaken. Integral calculations are implemented on each generic element of the discretized problem domain. The resulting systems of nonlinear equations are solved efficiently because of the coefficient matrix sparsity to yield both the dependent variable and its flux. In order to validate the formulation, the effects of the thermogeometric parameter, nonlinearity due to the temperature-dependent thermal conductivity, and of the heat transfer coefficient on the fin temperature distribution are investigated. The results are found to be in agreement with those for similar problems described in the literature and with the physics of the problem.

Keywords: *convective heat transfer, longitudinal fin, temperature-dependent thermal conductivity, systems of nonlinear equations, discretized problem domain, sparsity of coefficient matrix, integral calculations, generic element, thermogeometric parameter.*

Introduction. The primary challenge in handling a second-order ordinary differential equation for the fin problem is the presence of nonlinearity arising due to the temperature-dependent thermal conductivity. For considerably long longitudinal fins with uniform cross-sectional circular and rectangular geometries, the temperature variation is assumed to occur only in the axial direction. This consideration explains why most fin heat transfer calculations are one-dimensional and nonlinear, except for the cases when all the thermophysical properties, including the thermal conductivity, are assumed constant [1, 2]. However for most practical applications, the dependence of the heat transfer coefficient on a dependent variable should be expressed in such a way as to accurately represent the energy transfer process according to exponential, linear, or power law. A consideration of these factors with respect to heat transfer in a longitudinal fin constitutes the primary motivation for this study. In addition, we have extended our investigation to include the cases of internal heat generation occurring in current carrying electric arcs, nuclear rods, or any other heat generating components.

The studies involving temperature-dependent thermal conductivity and heat transfer coefficient have for a long time provided a fertile ground for researches. Aziz and Benzies [3] applied a regular perturbation technique to study convective heat transfer in a fin with variable thermal conductivity. In a later study, Pakdemirli and Sahin [4] as well as Bokhari, Kara, and Zaman [5] obtained analytic solutions of the fin problem with variable thermal conductivity by the symmetry method. Mebine and Olali [6] applied the Leibnitz–MacLaurin method (LMM) for obtaining a series solution of the nonlinear fin equation. Their work showed that an increase in the thermal conductivity resulted in a rise in the wall temperature, whereas the opposite result took place with increasing thermogeometric parameter. Their LMM results showed excellent agreement with previous closed-form solutions. Semianalytic techniques, such as the homotopy analysis method (HAM), variational iteration method (VIM), differential transform method (DTM), homotopy perturbation method (HPM), Adomian decomposition method (ADM), and the more recent Leibnitz–MacLaurin method (LMM) gave solutions expressed in a series form because most if not all their algorithms are based on variants of the Taylor series expansion. Such solutions may not be as flexible as those obtained numerically, being often used as benchmarks for validating numerical ones. In this connection, mention may be made of the works by Coskun and Atay [7], Aziz and Enamul Hug [8], Campo and Spaulding [9], Kraus, Aziz, and Welty [10], Fatoorechi and Abolghasemi [11], Moitsheki [12], and Khani and Aziz [13].

Computational Science Program, Addis Ababa University, Arat Kilo Campus, Addis Ababa, Ethiopia; email: okuzaks@yahoo.com. Published in Inzhenerno-Fizicheskii Zhurnal, Vol. 93, No. 6, pp. 1629–1636, November–December, 2020. Original article submitted July 18, 2018; revision submitted February 26, 2020.

In other attempts, the domain-based numerical techniques were predominantly used. Sobamowo [14] applied the finite difference technique to solve systems of nonlinear equations resulting from the fin problem. His results showed that the fin temperature distribution, total heat transfer rate, and the fin efficiency were significantly determined by the thermophysical fin properties. He also found that an increase in the temperature-dependent thermal conductivity, as well as in internal heat generation, affects the thermal stability range of the computations. Similar attempts can be found in the work by Coskun and Atay [7]. A closer approach to the solution of the fin problem with variable thermal conductivity reveals a clear bias towards semianalytic solutions, except some few cases that involve domain discretization or decomposition (see the works by Arslanturk [15] and Chiu and Chen [16]). In the present work, we still retain domain discretization, but in addition with converting the governing differential equation into its integral analog. The resulting elemental equations are assembled and solved to yield the primary dependent variable as well as its flux at each node.

Mathematical Formulation. Figure 1 shows a straight fin attached to a heat source with temperature T_b that is placed in a fluid with temperature T_a. The insulated fin has an arbitrary cross-sectional area A, perimeter P, and length b. The one-dimensional energy balance is given as

$$A \frac{d}{dx}\left[K(T) \frac{dT}{dx}\right] - Ph(T - T_a) = 0 , \tag{1}$$

where $K(T)$ is the temperature-dependent thermal conductivity and h is the heat transfer coefficient. The thermal conductivity is assumed as

$$K(T) = k_a(1 + \lambda(T - T_a)) , \tag{2}$$

where k_a is the thermal conductivity of the ambient fluid and λ is the parameter determining the thermal conductivity variation. Equation (1) is nondimensionalized with the following variables:

$$\theta = (T - T_a)/(T_b - T_a) , \quad X = x/b , \quad \psi = [hPb^2/(k_a A)]^{0.5} , \tag{3}$$

where ψ is the dimensionless thermogeometric fin parameter. As a result, Eq. (1) can be presented in the following compact form:

$$\frac{d^2\theta}{dX^2} = -\frac{d \ln D(\theta)}{dX} \frac{d\theta}{dX} + \frac{\psi^2}{D(\theta)} \theta . \tag{4}$$

Here θ and X are the dimensionless temperature and coordinate, respectively, and $D(\theta)$ is the dimensionless temperature-dependent thermal conductivity given by $D(\theta) = 1 + \beta\theta$, where $\beta = \lambda(T_b - T_a)$ is the fin parameter which determines the variation of the temperature-dependent thermal conductivity. Equation (4) is a second-order dimensionless nonlinear differential equation with the following boundary conditions:

$$\left.\frac{d\theta}{dX}\right|_{X=0} = 0 , \quad \theta(1) = 1 . \tag{5}$$

The following variables are very relevant for studying the heat transfer process: the heat transfer rate expressed as

$$Q = \int_0^b P(T - T_a)\, dX \tag{6a}$$

and the fin efficiency equal to the ratio between the fin heat transfer rate and that calculated for the case as the entire fin is at the base temperature

$$\eta = \frac{Q}{Q_{ideal}} = \frac{\int_0^b P(T - T_a)\, dX}{Pb(T_b - T_a)} = \int_0^1 \theta(X)\, dX . \tag{6b}$$

The integral analog of Eq. (4) obtained via the Green second identity is

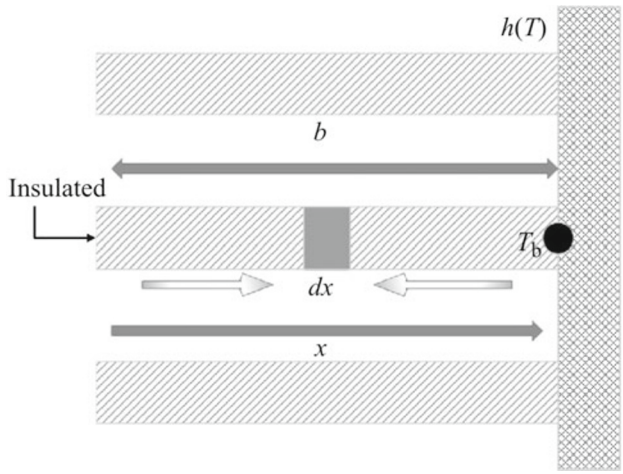

Fig. 1. Schematic diagram of the problem.

$$-2\lambda\theta_i + [H(X_2 - X_i) - H(X_i - X_2)]\theta_2 - [H(X_1 - X_i) - H(X_i - X_1)]\theta_1$$
$$- [|X_2 - X_i| + l_\mathrm{m}]\varphi_2 + [|X_1 - X_i| + l_\mathrm{m}]\varphi_1 + \int_{x_0}^{x_L} \left[- \frac{d \ln D(\theta)}{dX} \varphi + \frac{\psi^2}{D(\theta)} \right] dX = 0 , \quad i = 1, 2 , \tag{7}$$

where $H(X)$ is the Heaviside function, φ is the derivative of the dependent variable, x_0, x_L, and l_m are the x coordinates of the ends of an element in the problem domain and the maximum length. Equation (7) begins the process of converting a system of numerical approximations of a continuous differential equation into a finite number of discrete elemental equations in the problem domain. We formalize this procedure by representing Eq. (7) at each node of a linear element in the discretized problem domain.

At node 1 ($x_i = x_1$) we have

$$-\theta_1 + \theta_2 + l_\mathrm{m}\varphi_1 - (l_\mathrm{m} + l)\varphi_2 + \int_0^1 \left[(|X - X_1| + l_\mathrm{m})\Omega_j\varphi_j \left\{ - \frac{1}{l_\mathrm{m}} \frac{d\Omega_n}{dX} \Theta_n \right\} \right] dX$$
$$+ \int_0^1 [(|X - X_1| + l_\mathrm{m})\Omega_n\chi_n\Omega_j\{\psi^2\theta_j\}] \, dX = 0 , \quad j, n = 1, 2 ; \tag{8a}$$

similarly at node 2 ($x_i = x_2$)

$$\theta_1 - \theta_2 - l_\mathrm{m}\varphi_2 - (l_\mathrm{m} + l)\varphi_1 + \int_0^1 \left[(|X - X_1| + l_\mathrm{m})\Omega_j\varphi_j \left\{ - \frac{1}{l_\mathrm{m}} \frac{d\Omega_n}{dX} \Theta_n \right\} \right] dX$$
$$+ \int_0^1 [(|X - X_2| + l_\mathrm{m})\Omega_n\chi_n\Omega_j\{\psi^2\theta_j\}] \, dX = 0 . \tag{8b}$$

We approximate the quantities $\ln D(\theta) = \Theta$, $1/D(\theta) = \chi$, and $d\theta/dX = \varphi$ by linear functions. Now the system of discrete elemental equations can be cast in a representative matrix form as

$$R_{ij}\theta_j + (L_{ij} - \Lambda_{inj}\Theta_n)\varphi_j + \Psi_{inj}\chi_n(\psi^2\theta_j) = 0 , \quad i, j, n = 1, 2 . \tag{9}$$

Without loss of generality, we can use further advantage of this integral discrete domain-driven numerical procedure, assuming that the temperature-dependent thermal conductivity is uniform within each element, and present the resulting variable as

$$D(\theta) \approx D(\overline{\theta}) = D[(a\overline{\theta}^{k+1()} + b\overline{\theta}^{(k)})] , \quad 0 \le a \le 1 , \quad b = 1 - a , \tag{10}$$

where k is the iteration level, $\overline{\theta}^{(k+1)} = (\overline{\theta}_1^{(k+1)} + \overline{\theta}_2^{(k+1)})/2$ is the elemental average of the dependent variable at the current iteration level, $\overline{\theta}^{(k)} = (\overline{\theta}_1^{(k)} + \overline{\theta}_2^{(k)})/2$ is such the average at the previous iteration level, and the subscripts refer to the nodal numbers of each element. It should be mentioned that a uniform representation of the dependent variable within an element presents a noticeable simplification of Eq. (9) which can be presented as

$$R_{ij}\theta_j + L_{ij}\varphi_j + \Upsilon_{ij}\overline{\chi}(\psi^2\theta_j) = 0 . \tag{11}$$

Equation (11) is still nonlinear, and the Picard scheme is adopted for its linearization.

To illustrate the versatility of this elegant and straightforward approach, Eq. (1) is modified to include internal heat generation:

$$A\frac{d}{dx}\left[K(T)\frac{dT}{dx}\right] - Ph(T_b - T_a) + Q_{int}(T) = 0 . \tag{12}$$

After the same dimensionalization procedure, Eq. (12) looks like:

$$\frac{d^2\theta}{dX^2} = -\frac{d\ \ln\ D(\theta)}{dX}\frac{d\theta}{dX} + \frac{\psi^2}{D(\theta)}(\theta - Q\{1 + z\theta\}) , \tag{13}$$

where z is the dimensionless internal heat generation parameter. The boundary condition is still presented by Eq. (5). Finally Eq. (13) becomes:

$$R_{ij}\theta_j + L_{ij}\varphi_j + \Upsilon_{ij}\overline{\chi}\psi^2(\theta_j + Q\{1 + z\theta_j\}) = 0 . \tag{14}$$

Equations (11) and (14) show that the flux term is computed directly as a second dependent variable, hence the accuracy of its determination is directly linked to the scalar profile. For this reason, the flux is handled in such a way as to enhance stability and reduce any intermodal flux discontinuities and unphysical oscillations, especially for high-gradient problems or for the problems where scalar quantities must remain positive for some physical reasons. As a result we get

$$-\int_\Gamma G(X_i)\varphi\ ds = -\int_\Gamma G(X_i)\frac{dT}{dn}\ ds = \int_\Gamma G(X_i)\left(-D\frac{dT}{dn}\frac{1}{D}\right) ds = \int_\Gamma G(X_i)\frac{q}{D}\ ds , \tag{15}$$

where $q = -D\dfrac{dT}{dn}$. The quantity $\dfrac{q}{D}$ is approximated by a linear basis function, and now the flux term is given as

$$\int_\Gamma G(X_i)N_j\left(\frac{q}{D}\right) ds = L_{ij}\left(\frac{q}{D}\right) . \tag{16}$$

For the problem solved, D is a function of the dependent variable, and for each iteration it is presented through the previous iteration value

$$L_{ij}\left(\frac{q}{D}\right)_j = \left(\frac{L_{ij}}{D^{ik}}\right)(q_j) . \tag{17}$$

This procedure guarantees the achievement of conservation in an integral sense not only locally but globally, as well as because of the interaction between the adjacent nodes of an element in the problem domain by virtue of a shared boundary.

Numerical Results. Table 1 enables one to compare the results of the exact solution for the linear case ($\beta = 0$) obtained by the method developed herein with the analytical solution $\theta(X) = \cosh(\psi X)/\cosh\psi$ at $0 \le X \le 1$ and

TABLE 1. Dimensionless Temperature as a Result of Numerical and Exact Solutions in the Linear Case ($\beta = 0$)

X	$\psi = 0.5$		$\psi = 1$	
	Exact	Numerical (present)	Exact	Numerical (present)
0	8.87E–01	8.87E–01	6.48E–01	6.48E–01
0.1	8.88E–01	8.88E–01	6.51E–01	6.51E–01
0.2	8.91E–01	8.91E–01	6.61E–01	6.61E–01
0.3	8.97E–01	8.97E–01	6.77E–01	6.77E–01
0.4	9.05E–01	9.05E–01	7.01E–01	7.01E–01
0.5	9.15E–01	9.15E–01	7.31E–01	7.31E–01
0.6	9.27E–01	9.27E–01	7.68E–01	7.68E–01
0.7	9.41E–01	9.42E–01	8.13E–01	8.13E–01
0.8	9.61E–01	9.59E–01	8.69E–01	8.67E–01
0.9	9.86E–01	9.78E–01	9.37E–01	9.29E–01
1.0	1.00E+00	1.00E+00	1.00E+00	1.00E+00

TABLE 2. Dimensionless Temperature as a Result of Numerical and Semianalytic (HAM) Solutions in Nonlinear Cases

X	$\beta = 0.5$, $\psi = 1$		$\beta = 0.2$, $\psi = 0.5$	
	HAM	Numerical (present)	HAM	Numerical (present)
0	6.48E–01	6.48E–01	9.03E–01	9.04E–01
0.1	6.51E–01	6.51E–01	9.04E–01	9.05E–01
0.2	6.61E–01	6.61E–01	9.07E–01	9.08E–01
0.3	6.77E–01	6.77E–01	9.12E–01	9.13E–01
0.4	7.01E–01	7.01E–01	9.19E–01	9.19E–01
0.5	7.31E–01	7.31E–01	9.27E–01	9.28E–01
0.6	7.68E–01	7.68E–01	9.38E–01	9.38E–01
0.7	8.13E–01	8.13E–01	9.51E–01	9.51E–01
0.8	8.69E–01	8.67E–01	9.65E–01	9.67E–01
0.9	9.37E–01	9.29E–01	9.82E–01	9.94E–01
1.0	1.00E+00	1.00E+00	1.00E+01	1.00E+00

$\psi = 0.5$ and 1. Table 2 gives the results for nonlinear cases ($\beta \neq 0$) at different values of the thermogeometric parameter β. Good agreement of the analytic and numerical results is observed in all the cases. Figure 2a illustrates the effect of the value of the thermal conductivity parameter β on the dimensionless temperature profile for a fixed value of the thermogeometric parameter ψ. The nonlinear temperature increase with increasing β is seen. Figure 2b shows the dimensionless temperature profiles for the linear case ($\beta = 0$) and different values of the thermogeometric parameter ψ. It is observed that as ψ increases (i.e., the fin length increases or the cross-sectional area decreases), a lesser temperature is recorded.

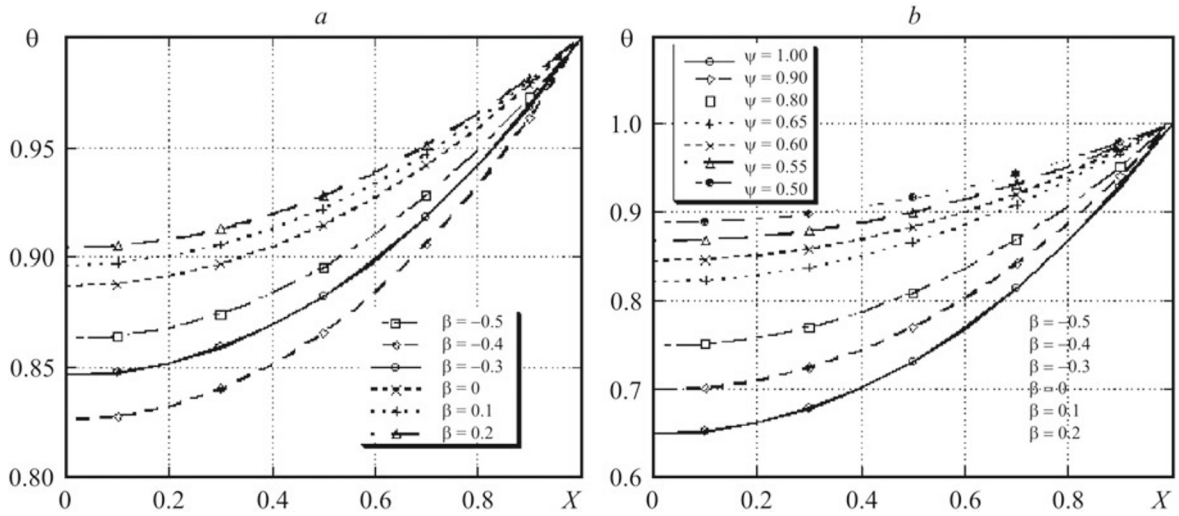

Fig. 2. Dimensionless temperature profiles: at $\psi = 0.5$ and different values of β (a); at $\beta = 0$ and different values of ψ (b).

TABLE 3. Dimensionless Temperature with Heat Generation as a Result of Numerical and Analytic Solutions in the Linear Case ($\beta = 0$) at $\gamma = 0.3$

X	$Q = 0.3$, $\psi = 0.5$		$Q = 0.5$, $\psi = 1.0$	
	Analytic	Numerical (present)	Analytic	Numerical (present)
0	8.87E–01	8.87E–01	6.48E–01	6.48E–01
0.1	8.88E–01	8.88E–01	6.51E–01	6.51E–01
0.2	8.91E–01	8.91E–01	6.61E–01	6.61E–01
0.3	8.97E–01	8.97E–01	6.77E–01	6.77E–01
0.4	9.05E–01	9.09E–01	7.01E–01	7.01E–01
0.5	9.15E–01	9.21E–01	7.31E–01	7.31E–01
0.6	9.27E–01	9.34E–01	7.68E–01	7.68E–01
0.7	9.42E–01	9.50E–01	8.14E–01	8.13E–01
0.8	9.59E–01	9.68E–01	8.67E–01	8.67E–01
0.9	9.79E–01	9.78E–01	9.29E–01	9.29E–01
1.0	1.00E+00	1.00E+00	1.00E+00	1.00E+00

We are coming now to the cases involving internal heat generation. Table 3 shows very close agreement between the analytic and numerical results. Figure 3a displays the profiles of the dimensionless temperature along the fin for $\beta = 0.2$, $Q = 0.3$, and $z = 0.5$. It is seen that the profiles become steeper and the temperature decreases with increase in ψ. This behavior is due to the fact that ψ is proportional to the fin length. In addition, it is observed that relatively small values of ψ may lead to unstable heat transfer in the fin. Figure 3b shows that an increase in the thermal conductivity parameter β increases the heat transfer rate through the fin within the constraints established by the fixed values of the fin parameter and internal heat generation. This is primarily due to the fact that, as this takes place, both the dimensionless fin temperature and the heat transfer rate increase. Similar trends can be observed in Fig. 3c and d for increase in the dimensionless temperature

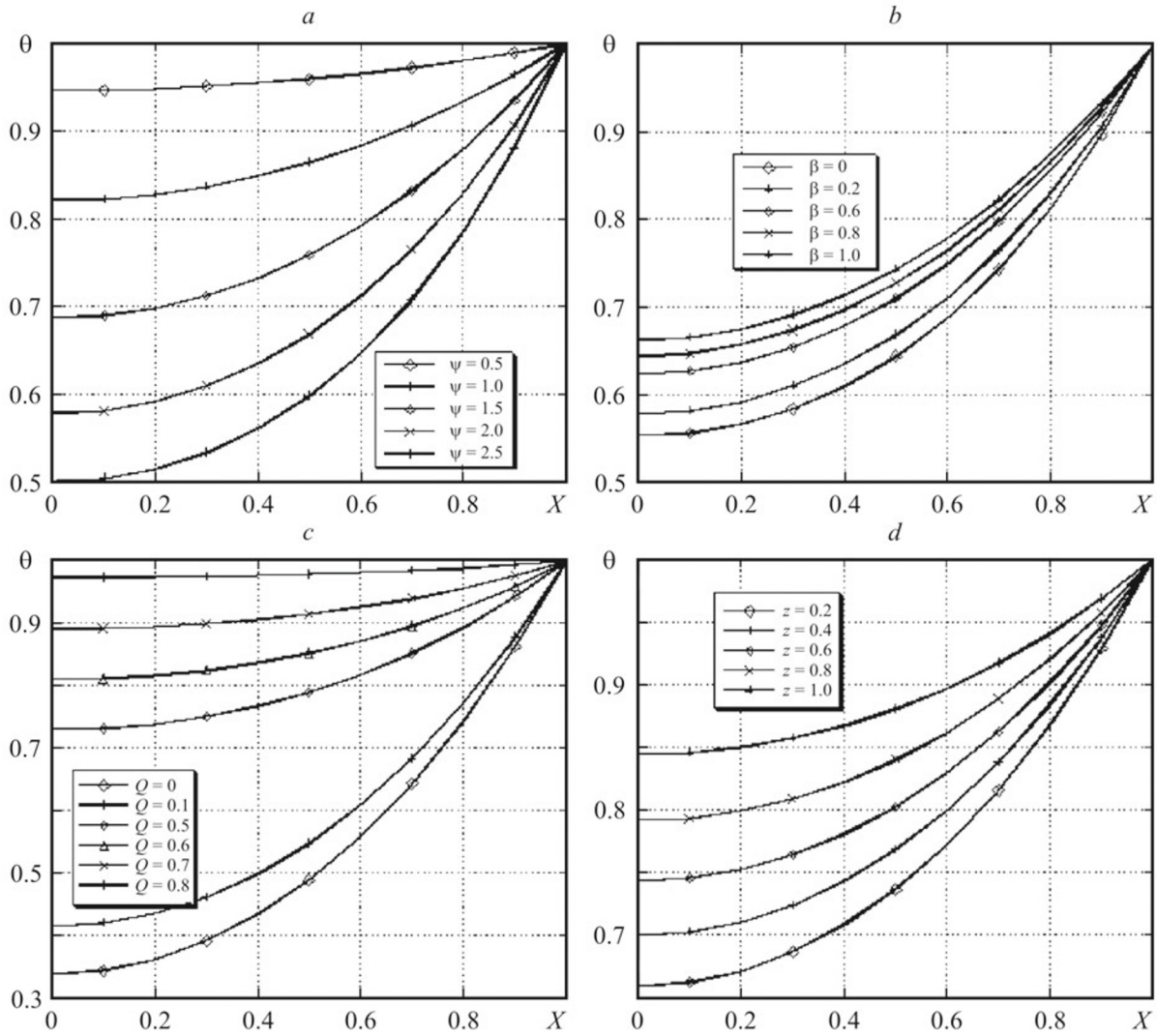

Fig. 3. Dimensionless temperature profiles: at $z = 0.5$, $Q = 0.3$, $\beta = 0.2$, and different values of ψ (a); at $z = 0.6$, $Q = 0.3$, $\psi = 2$, and different values of β (b); at $z = 0.2$, $\psi = 2$, $\beta = 0.5$, and different values of Q (c); at $\psi = 2$, $\beta = 0.6$, $Q = 0.4$, and different values of z (d).

with the dimensionless heat transfer rate and internal heat generation parameter, respectively. As the internal heat generation parameter increases, the fin efficiency for fixed fin parameters rises.

The computational scheme developed herein is further tested to see how accurately it can predict the flux [see Eq. (17)]. Figure 4a shows that the smallest flux is observed for $\beta = 0$ and it rises with β, reaching the maximum value at $\beta = 1$. We also note that all the flux values are equal to zero at $X = 0$. This is in accordance with the specified boundary condition as well as with the physics of the problem. Figure 4b illustrates the effect of the Biot number on the flux profile for a fixed set of the fin parameters. As mentioned in [14], this number for the one-dimensional fin analysis should lie within $0 < \mathrm{Bi} < 0.1$, otherwise the two-dimensional analysis is recommended. It can be observed that the higher is the Biot number, the lower is the predicted flux. Since the Biot number mimics the thermogeometric parameter ψ, because both of them depend on the fin length, an interesting comparison between the fin flux profiles in Fig. 4b and the fin temperature profiles in Fig. 3a is worthy of attention. In both cases the highest value of the dimensionless characteristic is matched by the lowest value of the corresponding parameter. This relates especially to the thermogeometric parameter: the smaller is this parameter, the less stable is the fin heat transfer computation.

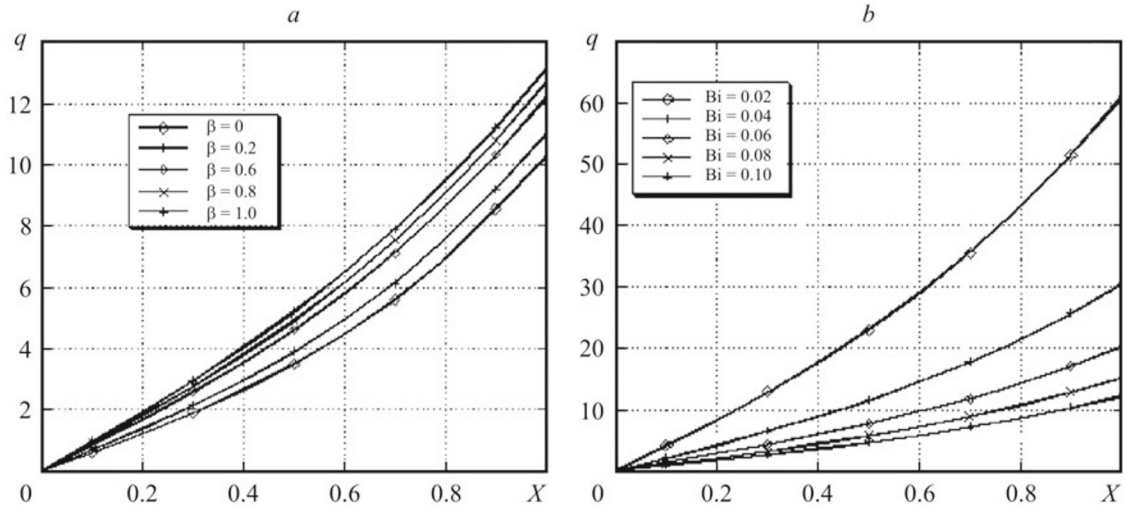

Fig. 4. Dimensionless flux profiles for $Q = 0.4$ and $z = 0.2$: at $\psi = 0.2$ and different values of β (a); at $\psi = 2$, $\beta = 0.6$, and different values of Bi (d).

Conclusions. The problem of heat transfer in a fin with temperature-dependent thermal conductivity has been considered. This nonlinear problem has been solved by converting the governing nonlinear second-order differential equation into its integral analog. The resulting integral equations for each element were assembled and solved to yield the primary dependent variable as well as its flux for each node of a linear element in the problem domain. These results were compared, where possible, with the available closed-form solutions or numerical ones for the same problem. A comparison not only showed good agreement, but also has demonstrated that this formulation can be relied on to produce satisfactory results with considerable little numerical efforts. An additional point is the fact that this work can initiate researches that address the paucity of information on integral calculations involving the fin problems.

NOTATION

A, cross-sectional area; Bi, Biot number; b, length; D, dimensionless thermal conductivity; h, heat transfer coefficient; $K(T)$ and k_a, thermal conductivity of the fin and ambient fluid; P, perimeter; Q, heat transfer rate; q, heat flux; T_a, T_b, temperatures of the fluid and heat source, respectively; T, fin temperature; x, coordinate; X, dimensionless coordinate; z, dimensionless internal heat generation parameter; θ, dimensionless temperature; ψ, thermogeometric fin parameter.

REFERENCES

1. D. Q. Kern and A. D. Kraus, *Extended Surface Heat Transfer*, McGraw-Hill, New York (1972).
2. Y. Cengel and A. Ghajar, *Heat and Mass Transfer: Fundamentals and Applications*, McGraw-Hill, New York (2011).
3. A. Aziz and J. Y. Benzies, Application of perturbation techniques to heat transfer with variable thermal properties, *Int. J. Heat Mass Transf*., **19**, 271–276 (1976).
4. M. Pakdemirli and A. Z. Sahin, Similarity analysis of a nonlinear fin equation, *Appl. Math. Lett*., **19**, 378–384 (2006).
5. A. H. Bokhari, A. H. Kara, and F. D. Zaman, A note on symmetry analysis and exact solutions of a nonlinear fin equation, *Appl. Math. Lett*., **19**, 1356–1360 (2006).
6. P. Mebine and N. Olali, Leibnitz–MacLaurin method for solving temperature distribution in straight fins with temperature dependent thermal conductivity, *J. Sci. Eng. Res*., **3**, No. 2, 97–105 (2016).
7. S. B. Coskun and M. T. Atay, Fin efficiency analysis of convective straight fins with temperature dependent thermal conductivity using variational iteration method, *Appl. Therm. Eng*., **28**, 2345–2352 (2008).
8. A. Aziz and S. M. Enamul Hug, Perturbation solution for convecting fin with variable thermal conductivity, *ASME J. Heat Transf.*, **97**, 300–301 (1975).
9. A. Campo and R. J. Spaulding, Coupling of methods of successive approximations and undetermined coefficients for the prediction of thermal behavior of uniform circumferential fins, *Heat Mass Transf*., **25**, No. 6, 461–468 (1999).

10. A. D. Kraus, A. Aziz, and J. Welty, *Extended Surface Heat Transfer*, Wiley, New York (2001).
11. H. Fatoorechi and H. Abolghasemi, Investigation of nonlinear problems of heat conduction in tapered cooling fins via symbolic programming, *Appl. Appl. Math.: An Int. J.*, **7**, No. 2, 717–734 (2012).
12. R. J. Moitsheki, Steady one-dimensional heat flow in a longitudinal triangular and parabolic fin, *Commun. Nonlinear Sci. Numer. Simul*., **16**, 3971–3980 (2011).
13. F. Khani and A. Aziz, Thermal analysis of a longitudinal trapezoidal fin with temperature dependent thermal conductivity and heat transfer coefficient, *Commun. Nonlinear Sci. Numer. Simul.*, **15**, 590–601 (2010).
14. M. G. Sobamowo, Analysis of convective longitudinal fin with temperature dependent thermal conductivity and internal heat generation, *Alexandria Eng. J*., **56**, 1–11 (2017).
15. A. Arslanturk, A decomposition method for fin efficiency of convective straight fin with temperature dependent thermal conductivity, *Int. Commun. Heat Mass Transf*., **32**, 831–841 (2005).
16. Ching-Huang Chu and Chao-Kung Chen, A decomposition method for solving the convective longitudinal fins with variable thermal conductivity, *Int. J. Heat Mass Transf*., **45**, 2067–2075 (2002).